Sol−Gel Derived Gold Nanoclusters in Silica Glass Possessing Large Optical Nonlinearities

S. Tamil Selvan,*,†,‖ Tomokatsu Hayakawa,† Masayuki Nogami,† Yoshio Kobayashi,‡ Luis M. Liz-Marzán,‡ Yasushi Hamanaka,§ and Arao Nakamura§

Department of Materials Science & Engineering, Nagoya Institute of Technology, Gokiso-cho, Showa-ku, Nagoya 466-855, Japan, Departamento de Química Física, Universidade de Vigo, E-36200, Vigo, Spain, and Department of Applied Physics, Faculty of Engineering, Nagoya University, Chikusa-ku, Nagoya 464-8603, Japan

Received: April 1, 2002; In Final Form: July 12, 2002

Sol−gel derived gold/silica glasses, starting with Au sols prepared by two different methodologies, one without the aid of any external stabilizing agent and the other with silica-coated Au, are described. The optical absorption spectra show the typical surface plasmon resonance for Au at around 520−530 nm. Transmission electron microscopy reveals the existence of spherical Au particles in the silica matrix. The mean diameters of Au nanoclusters in gels and glasses vary from 10 to 20 nm and from 27 to 38 nm, respectively, supported by X-ray diffraction data. The third-order optical nonlinearities $|\chi^{(3)}|$ determined by a degenerate four-wave mixing (DFWM) method exhibit a higher value of 2.2×10^{-9} esu for a glass with 0.5 wt % Au heated at 600 °C indicating that a larger size induces an enhancement effect. This method also offers a greater $\chi^{(3)}/\alpha$ (α: absorption coefficient) value of 1×10^{-11} esu cm, which is comparable to those values obtained by a sputtering method. Thus, these novel $Au-SiO_2$ nanocomposites fabricated by facile sol−gel methods render them potential candidates for photonic applications.

Introduction

Metal or semiconductor nanoclusters dispersed in a transparent matrix such as glasses, have high resonant type third-order optical nonlinearity $|\chi^{(3)}|$.[1] Nanometer dimension metal particle−glass composites exhibit not only a large third-order nonlinear response, but also picosecond switching and relaxation times, thermal and chemical stability, high laser damage threshold, low photon absorption and tunability.[2] Metal nanoparticles dispersed in a dielectric medium have a unique optical effect called surface plasmon resonance (SPR), which serves as the basis for high third-order optical nonlinear susceptibility.[3] The significant feature of SPR is the enhancement of an electric field of light near the metal particles. The SPR can enhance any kind of photoexcitation processes occurring near the metal particles through electrical field enhancement as long as the photoexcitation and SPR occur at the same wavelength.[4] Third-order optical nonlinearity is a typical example, where the nonlinear optical process is enhanced by SPR. Surface-enhanced Raman scattering (SERS) was characterized by SPR for a range of organic molecules.[3a] We have recently demonstrated the enhancement of fluorescence from lanthanide ions, near metal or semiconductor nanoparticles, doped in silica gels and glasses.[5] Very recently, SERS studies of semiconductor−semiconductor (CdS/CdSe) superlattice films formed on gold by electrochemical atomic-layer epitaxy (ECALE) have been described in the literature.[6] Nonlinear optical effects have also been observed in layer-by-layer assembled films of magnetic[7] and metallic nanoparticles,[8] though in the latter case the authors mention possible interactions affecting the optical nonlinearities.

Sol−gel optics is becoming a major field of sol−gel science because the sol−gel process offers unique opportunities for the synthesis of optical materials in the form of thin films, fibers, fine powders, and even monoliths.[9] The homogeneous mixing of several components at a molecular level makes it possible to vary the chemical nature of optical materials over a wide range of compositions in order to tailor their optical properties. The formation of metal colloids by the controlled reduction of metal salts, nucleation, and growth in aqueous solution has been investigated since the days of Faraday in 1857.[10] Much of the interest in gold colloids stems from their remarkable stability, monodispersity, and interesting optical properties. Importantly, optical properties of Au nanocrystals embedded in polymers[11] have been widely studied owing to their linear and nonlinear characteristics.

To stabilize the Au nanoparticles in silica gels either amino-functionalized sol−gel monomers or a stabilizing agent should be employed. Organo-functionalized silanes have been used for stabilizing Au nanoparticles in sol−gel films and coatings.[12,13] The preparation of gold colloids using tetraethoxysilane (TEOS) or methyltrimethoxysilane (MTMOS) in the absence of aminosilane precursors resulted in the immediate aggregation of the Au particles during reduction with $NaBH_4$.[14] Recently, we have shown the preparation of the polymer-protected Au particles in a silica glass[15] and a facile method of encapsulating Au nanoparticles in a silica gel without the aid of any external stabilizing agent.[16] We have also reported the synthesis of novel gold−silica core−shell particles,[12a,b] and their incorporation within silica gels.[12c] In this paper, we discuss in detail the potentially important method of synthesizing Au nanoparticles isolated in silica gels (∼10−20 nm) and glasses (∼27−38 nm) and their nonlinear optical properties. It provides a simplified

* Corresponding author. Fax: +61-3-9347-5180. E-mail: tamil@unimelb.edu.au.

† Nagoya Institute of Technology.

‡ Universidade de Vigo.

§ Nagoya University.

‖ Present address: Nanotechnology Laboratory, Chemistry School, University of Melbourne, Parkville, Victoria 3010, Australia.

10.1021/jp020860x CCC: $22.00
Published on Web 09/07/2002

processing method that uses tetramethoxysilane (TMOS) directly, with no cosolvent and no need for functionalized silanes. We compare this method with the one based on an initial stabilization of the Au nanoparticles by silica coating and then incorporation into silica gels, which also provides high nonlinear optical susceptibility. The large third-order nonlinear optical susceptibility divided by the absorption coefficient ($\chi^{(3)}/\alpha$) of the composite material obtained by these approaches, in comparison with existing sputtering and ion implantation techniques, could open up new avenues in the field of photonics.

Experimental Section

A. Fabrication of Gold−Silica Composites through Method 1. Gold−silica composites (Au/SiO_2, 0.1 to 1.0 wt % Au) were fabricated according to the following method. The different gold concentrations in the gel were obtained by varying the concentration of the gold sol. First, Au hydrosol was prepared by mixing X cm^3 ($X = 0.4$, 2, and 4 for 0.1, 0.5, and 1 wt % Au, respectively) of a 25 mM $HAuCl_4$ aqueous solution with partially hydrolyzed tetrakis(hydroxymethyl) phosphonium chloride (THPC). The latter was prepared by adding 1 mL of a fresh 50 mM solution of THPC in water to 47 mL of 6.38 mM NaOH solution.[17] TMOS (5 mL) was slowly added dropwise into the homogeneous Au sol with vigorous stirring for 1 h and then 1.5 g of 0.15 M ammonia was added. The solution was stirred heavily for 5−10 min and the resulting homogeneous solution was transferred into polystyrene containers. A wet gel (light brown in color) formed within 20 min of ammonia addition. Drying at room-temperature resulted in stiff gels after 3−4 weeks. Glass samples were obtained by heating the dried gels at temperatures ranging from 600 to 800 °C at a heating rate of 50 °C an hour in air.

B. Gold−Silica Composites through Method 2. Silica-coated Au nanoparticles ($Au@SiO_2$) were prepared by the method previously reported.[12] Typically, a gold sol was prepared by boiling 5×10^{-4} M $HAuCl_4$ in the presence of 1.6×10^{-3} M sodium citrate.[18] This resulted in a stable dispersion of gold particles with an average diameter of around 15 nm, and 10% polydispersity. A freshly prepared aqueous solution of APS (2.5 mL, 1 mM) was added to 500 mL of the gold sol under vigorous magnetic stirring. The mixture of APS and gold dispersion was allowed to stand for 15 min and then 20 mL of a 0.54 wt % sodium silicate solution at pH 11 (adjusted with a cation-exchange resin) was added under vigorous magnetic stirring. The resulting dispersion (pH 8.5) was then allowed to stand for one week, so that the active silica polymerizes onto the primed gold particle surface. The silica shell was then about 5−7 nm thick. The Au concentration was adjusted by centrifugation at 3000 rpm for several hours and removal of supernatant. This also resulted in removal of excess sodium silicate from solution.

In a typical sol−gel procedure, first 0.32 mL of TMOS was added to 1.33 mL of methanol. Next, 2 mL of the nanoparticle dispersion was added to the mixture of TMOS and methanol. The final molar ratio of TMOS, water, and methanol was 1:50:15, assuming that 2 mL of colloid contained 2 mL of water. The final mixture was poured in a Petri dish, shielded with a rubber sheet to avoid rapid evaporation of the solvent. After several hours of drying, the shield was removed. Drying at room temperature for 3−4 weeks resulted in a xerogel. The dried gels were fired at 600 °C to obtain glasses.

C. Characterization of the Composites by BET, UV−Vis, TEM, and XRD. The pore characteristics such as specific surface area and pore volume of gels and glasses were acquired with a fully automated Quantachrome Corporation NOVA- 1000 surface area analyzer, and with a Micromeritics TriStar 3000 instrument at a constant temperature of 77.35 K. UV−Vis spectra measurements were carried out with a U-Best Spectrophotometer. The diameter of Au particles in gels and glasses was directly examined by transmission electron microscopy. TEM images were acquired with a JEOL-2000FX electron microscope, and a Philips CM20 electron microscope operating at 200 kV. The samples were prepared by mixing ground pieces of the gel or glass with ethanol and dropping the solution onto a carbon-coated Cu grid with an underlying tissue paper, leaving behind a thin film.

The X-ray diffraction (XRD) measurements were carried out with a Rigaku Rad-B system and a Siemens D-5000, to investigate the crystallinity and the mean diameter of Au particles. The mean diameter, d, was estimated using the Scherrer's equation,

$$d = 0.9\lambda/\beta \cos\theta \tag{1}$$

where λ is the wavelength of X-ray source and β (rad) the full width at half-maximum (fwhm) of the X-ray diffraction peak at the diffraction angle θ.

D. Nonlinear Optical Properties of Au/SiO_2 Gel/Glass. The third-order nonlinear susceptibility, $|\chi^{(3)}|$ was measured by a degenerate four-wave mixing (DFWM) method at room temperature. The light source was an excimer-laser-pumped dye laser with a pulse duration of 20 ns, a spectral width of 0.2 cm^{-1}, and a maximum peak power of 1 MW cm^{-2}. The value of $|\chi^{(3)}|$ was estimated by the following equation:

$$\chi^{(3)} = (n^2 c\lambda/32\pi^3)\,[\alpha/(1-T)T^{0.5}]\,(\eta^{0.5}/I_0) \tag{2}$$

where λ is the wavelength of incident light, α the absorption coefficient, T the transmissivity, η the diffraction efficiency, n the refractive index, and c the light velocity. η is defined by the intensity ratio of the signal beam I_s to the incident beam I_0. The value of $|\chi^{(3)}|$ is obtained from the measurement of the intensities of incident, transmitted, and signal beams.

Results and Discussion

A. Pore Characteristics, Optical Absorption, and Surface Characterization of Au/SiO_2 Composites. The room-temperature dried gels were violet or red in color, depending on the low (0.1) or high (1.0) weight percent of Au encapsulated in silica. The pore volume, pore radius, and surface area estimated from BET measurements for a typical sample of 0.5 wt % Au are found to be 0.576 mL/g, 22.83 Å, and 480.56 m^2/g, respectively. The surface area of glass samples with 0.7 wt % Au heated at 800 °C decreases to a value of 220.99 m^2/g. On the other hand, the pore radius is increased to 45 Å, which is well illustrated by the collapse of the pores at high temperature. The shrinkage of the gels was about 45 to 50%. The porosity was ~53%.

Figure 1, parts A and B, show the absorption spectra of Au-doped silica gels and glasses at different weight percents, prepared by methods 1 and 2, respectively. In Figure 1A, for low weight percent (0.1 wt % Au), the surface plasmon resonance is noticed at around 530 nm. In general, an increase in particle size is characterized either by a red shift or a sharper peak in the absorption spectra. The latter is apparent in our samples with a higher concentration of Au (dotted lines), so that for 1 wt % the full width at half-maximum (fwhm) decreases from 70 to 52 nm upon gel−glass transformation. On the other hand, gel samples (solid lines) show a broader

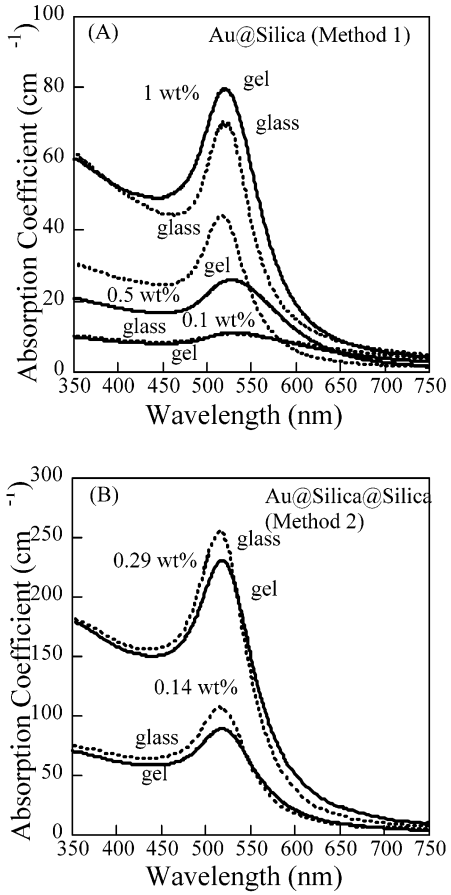

Figure 1. UV-Vis spectra of Au-doped silica gels and glasses prepared by method 1 (A) and method 2 (B). Au composition is given in weight percentage. The surface plasmon resonance for Au ranges from 520 to 526 nm for method 1 and 514 nm to 516 nm for method 2. The increase in particle size at higher concentration of Au is characterized by sharper peaks (dotted traces).

surface plasmon resonance, which is typical of smaller size clusters with a broader size distribution. It is interesting to note that the surface plasmon resonance for Au at 0.5 wt % (method 1) decreases from 526 to 520 nm for gel−glass transition (with a decrease in fwhm from 120 to 60 nm), whereas at 0.29 wt % Au (method 2) the absorption peak decreases from 516 to 514 nm (with a decrease in fwhm from 88 to 76 nm). The characteristic surface plasmon resonance of Au particles shifts from a broad resonance to sharper ones, when the heating temperature is increased. An increase in particle size is noticed, as the heat-treatment induces the agglomeration of Au particles, especially through method 1. In the case of method 2, an initial silica coating appears to protect the particles from aggregation during gel−glass transition, as indicated by a small shift (1−2 nm) and narrowing (6−8 nm) in surface plasmon resonance for Au particles.

Figure 2 depicts the DTA and TG curves for Au/SiO_2 gel with 1 wt % Au. The DTA endothermic behavior is noticed from ca. 28 to 175 °C. The TG curve illustrates the fact that the weight of the silica gel decreases with an increase in temperature until about 160 °C. The weight loss is ca. 5% at 160 °C, which is primarily due to the removal of water and methanol, resulting in condensation to a denser gel. X-ray photoelectron spectroscopic studies of Au/SiO_2 gels with 1 wt % Au showed a binding energy at ca. 83 eV, characteristic of Au ($4f_{7/2}$) corresponding to metallic gold (Au° state).[19] Furthermore, Si (2p) and O (1s) electron spectra showed the

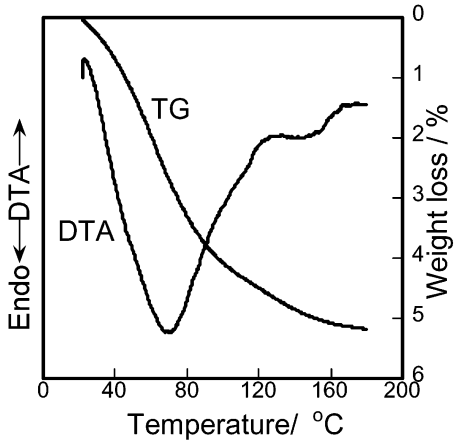

Figure 2. Typical DTA and TG curves of Au/SiO_2 gel with 1 wt % Au (method 1).

characteristic binding energies at 102 and 532 eV, respectively, which confirmed the formation of silica.

Shown in Figure 3 are representative TEM images of Au-doped silica gels (0.6 wt % Au) prepared by methods 1 and 2 and the average particle sizes are 18 and 15 nm, respectively. Yazawa et al. have reported a similar sol−gel process with ca. 50 nm Au particles in silica gels.[20] Furthermore, the photoreduction of $AuCl_4^-$ ions in sol−gel derived silica gels yielded particles with a larger size distribution and the particle sizes ranged from 25 to 170 nm for Au/SiO_2 gel with 1 wt % Au.[21] The novelty of our work is the relatively small particle size and the ability to increase concentration up to 1 wt % without significant aggregation. The reason for the lack of agglomeration is presumably simply a consequence of effective encapsulation of the Au particles in the silica matrix. As for method 2, initial silica-coated Au particles maintained their discrete nature even after gelation, as shown in micrograph (Figure 3b). In Figure 4 we show the TEM pictures for glass samples with 0.5 and 1 wt % Au heated at 800 °C. As can be seen the distribution of Au particles are wide and the mean diameters of Au for Au/SiO_2 glass with 0.5 and 1 wt % are 27 and 38 nm, respectively, which supports the absorption spectra shown in Figure 1A.

The powder XRD patterns of Au/SiO_2 gels at two different Au weight percents are shown in Figure 5A. The broad amorphous halo pattern at around $2\theta = 23°$ confirms the formation of silica. Sharp crystalline peaks are noticed at ca. $2\theta = 38°$ and 44°. These reflections are assigned, respectively, to (111) and (200) planes of cubic Au.[19] The Au particle size is estimated using the Scherrer's equation and found to be about 21 nm from the diffraction band at $2\theta = 38°$ in the case of 1 wt % Au. For the glass sample with 0.5 wt % Au the particle size is estimated to be ~26 nm (Figure 5b). Thus the XRD patterns indicate that a cubic Au−silica nanocomposite can be readily formed by both of these methods.

B. Nonlinear Optical Properties of Au/SiO_2 Composites. $\chi^{(3)}$ is expressed by the following equation using the third-order nonlinear susceptibility of a metal particle itself, $\chi_m^{(3)}$, and the local field factor $f_1(\omega)$,[22] where $f_1(\omega)$ is given by

$$\chi^{(3)} = pf_1(\omega)^2|f_1(\omega)|^2\chi_m^{(3)} \quad (3)$$

$$f_1(\omega) = 3\epsilon_d/[\epsilon_m(\omega) + 2\epsilon_d] \quad (4)$$

where ϵ_m and ϵ_d are the dielectric constant of the metal particle and matrix, respectively. At the plasmon resonance ($\omega \approx \omega_s$),

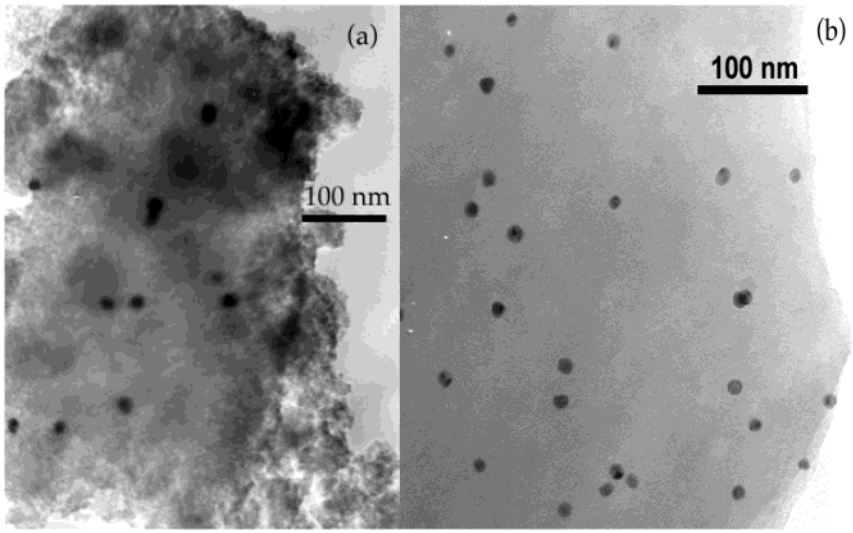

Figure 3. Transmission electron micrographs of Au-doped silica gels (Au/SiO_2: 0.6 wt %) prepared by methods 1 (micrograph a) and 2 (micrograph b). The mean particle diameters are 18 and 15, respectively.

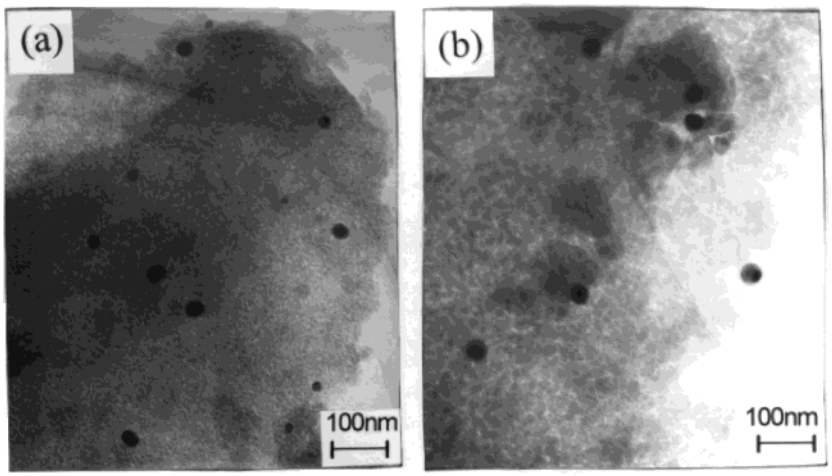

Figure 4. Transmission electron micrographs of Au-doped silica glass. Two different Au loading levels in glass (Au/SiO_2: 0.5 wt % and 1 wt %) are shown in (a) and (b). The mean particle diameters are 27 and 38 nm, respectively.

the following equation holds:

$$\epsilon_m'(\omega_s) + 2\epsilon_d(\omega_s) = 0 \tag{5}$$

$f_1(\omega_s)$ is then simply expressed by the following equation:

$$f_1(\omega_s) = 3\epsilon_d/\epsilon_m''(\omega_s) \tag{6}$$

The absorption coefficient in the vicinity of the surface plasmon resonance is given by

$$\alpha = p(\omega/nc)\, f_1(\omega)^2 \epsilon_m'' \tag{7}$$

where n is the refractive index of the matrix, c the light velocity, and p the volume fraction of particles. Accordingly, the following expression is obtained for $\chi^{(3)}/\alpha$:

$$\chi^{(3)}/\alpha = p(nc/\omega)\, f_1(\omega)^2 \chi_m^{(3)}/\epsilon_m''(\omega) \tag{8}$$

Assuming that $|\chi_m^{(3)}|$ is independent of particle size, $\chi^{(3)}/\alpha$ is proportional to $f_1\,(\omega)^2/\epsilon_m''(\omega)$. The value of $\epsilon_m''(\omega)$ can be easily obtained from the optical absorption spectra by using the analysis described in ref 21, and $f_1(\omega)$ is calculated using the value of $\epsilon_m''(\omega)$ by eq 4. The size-dependent behavior of $f_1(\omega)^2/\epsilon_m''(\omega)$ reasonably agreed with the measured $\chi^{(3)}/\alpha$. This suggested that the enhancement of the local field inside the particle gives rise to the size dependence of $\chi^{(3)}/\alpha$.[20] In our case, the value of $\chi_m^{(3)}$ was estimated to be 6.6×10^{-8} esu from eq 3. This value of $\chi_m^{(3)}$ is in reasonable agreement with the experimental values of $\chi_m^{(3)} = 4 \times 10^{-8} - 1 \times 10^{-7}$ esu.[23] The size-dependent enhancement of the $\chi^{(3)}$ in Au particles with the mean diameter of 11.0−37.0 nm has also been investigated. The value of $\chi^{(3)}/\alpha$ for the films increased with an increase of the mean diameter of Au particles. This is interpreted in terms of the size dependence of the local-field factor and the imaginary part of the dielectric constant of the metal particles. This size dependence effect has also been observed for Cu particles by Uchida et al.[24]

The third-order optical nonlinearity $|\chi^{(3)}|$ by the degenerate four-wave mixing method (DWFM) for gel samples with 0.1 wt % Au (method 1) and 0.14 wt % Au (method 2) showed values of 4.6×10^{-11} and 2.3×10^{-10} esu, respectively. These values are about 2 orders of magnitude larger than those of the silica gels doped with Au, reported by Yazawa et al. by a similar sol−gel method.[20] At higher Au concentrations, $\chi^{(3)}$ increases further, revealing that a larger size induces a larger effect. Table 1 depicts $\chi^{(3)}$ values of the composites. It is interesting to note that $\chi^{(3)}/\alpha$ for gel samples obtained by two different methods matches well (Table 1).

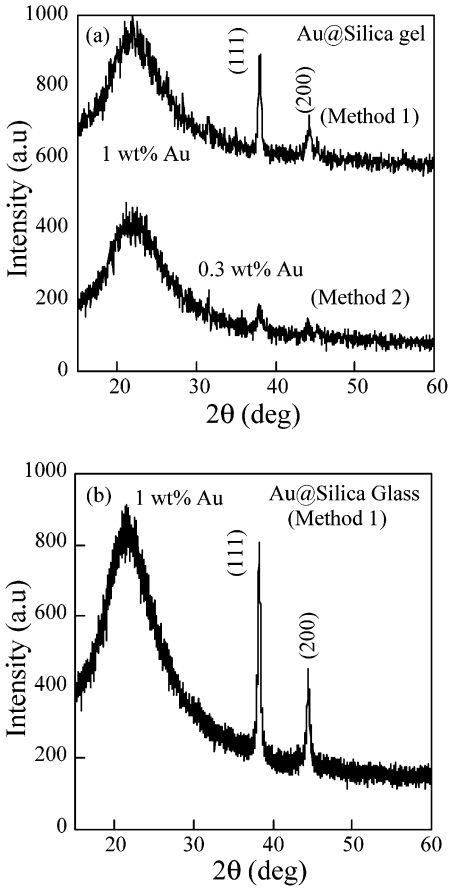

Figure 5. X-ray diffraction patterns of Au/SiO_2 gels (a) and glass (b). The broad amorphous pattern at around 23° confirms SiO_2. The characteristic (111) and (200) planes of cubic Au are noted.

TABLE 1: Third-order Optical Nonlinearities of Au/SiO_2 Gel/Glass Composites

Au/SiO_2 gel/glass	average particle size (nm)	$\chi^{(3)}$ (esu)	$\chi^{(3)}/\alpha$ (esu cm)
0.1 wt % gel at 25 °C (method 1)	11.1	4.6×10^{-11}	2.0×10^{-12}
0.1 wt % glass at 600 °C (method 1)	14.4	2.0×10^{-10}	5.2×10^{-12}
0.1 wt % glass at 800 °C (method 1)	16.3	7.3×10^{-10}	7.9×10^{-12}
0.5 wt % glass at 600 °C (method 1)	27.7	2.2×10^{-9}	1.0×10^{-11} [a]
0.3 wt % gel at 25 °C (method 2)	15.0	7.5×10^{-10}	4.2×10^{-12}
0.3 wt % glass at 600 °C (method 2)	15.0	4.6×10^{-10}	4.6×10^{-12}

[a] This high value is comparable to those obtained by a sputtering method delineated by Tanahashi et al.[22]

A glass sample with 0.5 wt % Au exhibits a higher value of 2.2×10^{-9} esu. This value is 2 orders of magnitude larger than those of Au particles in glasses prepared by the conventional melt-quenching method.[25] This is because the concentration of Au in the films is 2 orders of magnitude larger than that of the conventional glasses containing Au particles. The third-order nonlinear susceptibility of Au/SiO_2 thin films prepared by a sputtering method, exhibited a peak at the wavelength of the absorption peak and the maximum value of $\chi^{(3)}$ obtained was 2.0×10^{-7} esu.[22] When the particle size increases, $\chi^{(3)}$ also increases, as is evident in Table 1. In Figure 6, we show the dependence of $\chi^{(3)}$, $\chi^{(3)}/\alpha$, and the mean particle diameter of Au particles. Although the sputtering method produced high $\chi^{(3)}$,[22] the method presented here offers a greater $\chi^{(3)}/\alpha$, a figure of merit, which should be compared with regard to different preparative strategies. Compared to sputtering[22] and sol−gel dip coating,[26] our sol−gel method offers about five times greater $\chi^{(3)}/\alpha$ values.

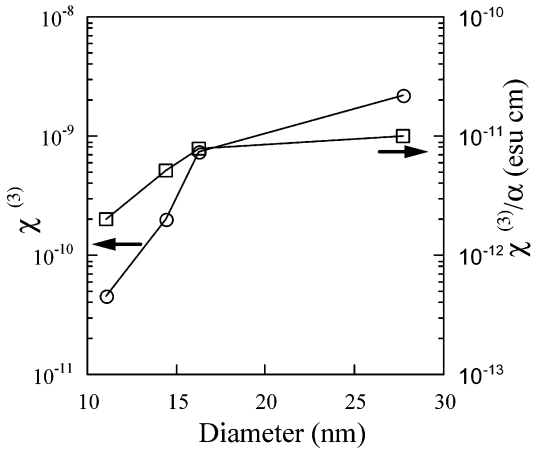

Figure 6. Dependence of $\chi^{(3)}$ and $\chi^{(3)}/\alpha$ on Au particle size.

Conclusions

In conclusion, we have characterized gold nanoclusters encapsulated within silica gels and glasses prepared either through a facile synthesis without the aid of any external stabilizing agent (method 1), or through sol−gel processing of silica-coated Au nanoparticles (method 2). The nonlinear optical properties of the composite materials have been studied in detail and compared for both systems. It was found that both methods allowed for the preparation of uniform composites with large third-order nonlinear optical susceptibilities. A figure of merit, $\chi^{(3)}/\alpha$ has been found to be greater than those of values reported by the sol−gel dip coating and sputtering methods.

Acknowledgment. S.T.S gratefully acknowledges the Japan Society for the Promotion of Science (JSPS) foundation, Tokyo and Venture Business Laboratory (VBL) of Nagoya Institute of Technology for financial support. Y.K. acknowledges the Spanish Ministerio de Educación y Cultura for a personal grant. L.M.L.M. acknowledges support from the Spanish Xunta de Galicia, (Project PGIDT01PXI30106PR) and Ministerio de Ciencia y Tecnología (Project. BQU2001-3799). J. Millos is thanked for performing for XRD measurements, and J.B. Rodríguez for TEM. We thank Paul Mulvaney for his valuable discussions.

References and Notes

(1) (a) Ricard, D.; Roussignol, Ph.; Flytzanis, Chr. *Opt. Lett.* **1985**, *10*, 511. (b) Dutton, T.; VanWonterghem, B.; Saltiel, S.; Chestony, N. V.; Rentzepis, P. M.; Shen, T. P.; Rogovin, D. *J. Phys. Chem.* **1990**, *94*, 1100. (c) Heolweil, E. J.; Hochestrasser, R. M. *J. Chem. Phys.* **1985**, *82*, 4762. (d) Kreibig, U.; Genzel, L. *Surf. Sci.* **1985**, *156*, 678. (e) Nogami, M.; Abe, Y. *J. Am. Ceram. Soc.* **1995**, *78*, 1066. (f) Kundu, D.; Honma, I.; Osawa, T.; Komiyama, H. *J. Am. Ceram. Soc.* **1994**, *77*, 1110. (g) Nogami, M. *Sol−Gel Optics: Processing and Application*; Kluwer: Boston, 1995; p 329. (h) Takada, T.; Yano, T.; Yasumori, A.; Yamane, M.; Mackenzie, J. D. *J. Non-Cryst. Solids* **1992**, *147&148*, 631.

(2) (a) Flytzanis, C.; Hache, F.; Klein, M. C.; Ricard, D.; Roussignol, P. H. *Progress in Optics*; Wolf, E., Ed.; North-Holland: Amsterdam, 1991; p 321. (b) Smith, P. W. *SPIE Proc.* **1993**, *1852*, 2. (c) Magruder, R. H., III; Weeks, R. A.; Morgan, S. H.; Pan, Z.; Henderson, D. O.; Zuhr, R. A. *J. Non-Cryst. Solids* **1995**, *192&193*, 546. (d) Wang, Y.; Herron, N. *J. Phys. Chem.* **1991**, *95*, 525.

(3) (a) Wokaun, A. *Mol. Phys.* **1985**, 56, 1. (b) Kozuka, H. *SPIE* **1997**, *3136*, 304.

(4) Nitzan, A.; Brus, L. E. *J. Chem. Phys.* **1981**, *75*, 2205.

(5) (a) Selvan, S. T.; Hayakawa, T.; Nogami, M. *J. Phys. Chem. B* **1999**, *103*, 7064. (b) Hayakawa, T.; Selvan, S. T.; Nogami, M. *Appl. Phys. Lett.* **1999**, *74*, 1513. (c) Selvan, S. T.; Hayakawa, T.; Nogami, M. *J. Non-Cryst. Solids* **2001**, *291*, 137.

(6) Zou, S.; Weaver, M. J. *Chem. Phys. Lett.* **1999**, *312*, 101.

(7) Murzina, T. V.; Nikulin, A. A.; Aktsipetrov, O. A.; Ostrander, J. W.; Mamedov, A. A.; Kotov, N. A.; Devillers, M. A. C.; Roark, J. *Appl. Phys. Lett.* **2001**, *79*, 1309.

(8) Schrof, W.; Rozouvan, S.; Van Keuren, E.; Horn, D.; Schmitt, J.; Decher, G. *Adv. Mater.* **1998**, *10*, 338.

(9) Brinker, C. J.; Scherer, G. W. *Sol−Gel Science*; Academic Press: New York, 1990.

(10) (a) Faraday, M. *Trans. Faraday Soc.* **1857**, 145. (b) Henglein, A. *Chem. Rev.* **1989**, *89*, 1861. (c) Schmid, G. *Chem. Rev.* **1992**, *92*, 1709. (d) Bradley, J. S.; Hill, E. W.; Behal, S.; Klein, C.; Chaudret, B.; Duteil, A. *Chem. Mater.* **1992**, *4*, 1234. (e) Kreibig, U.; Vollmer, M. *Optical Properties of Metal Clusters*; Springer: Berlin, 1995.

(11) (a) Chan, Y. N. C.; Schrock, R. R.; Cohen, R. E. *J. Am. Chem. Soc.* **1992**, *114*, 7295. (b) Antonietti, M.; Förster, S.; Hartmann, J.; Östreich, S. *Macromolecules* **1996**, *29*, 3800. (c) Röscher A.; Möller, M. *Adv. Mater.* **1995**, *7*, 151. (d) Spatz, J. P.; Mössmer, S.; Möller, M. *Chem. Eur. J.* **1996**, *2*, 1552. (e) Möller, M.; Spatz, J. P.; Röscher A.; Mössmer, S.; Selvan, S. T.; Klok, H.-A. *Macromol. Symp.* **1997**, *117*, 207. (f) Selvan, S. T.; Spatz, J. P.; Klok, H.-A.; Möller, M. *Adv. Mater.* **1998**, *10*, 132. (g) Selvan, S. T. *Chem. Commun.* **1998**, 351. (h) Selvan, S. T.; Hayakawa, T.; Nogami, M.; Möller, M. *J. Phys. Chem. B* **1999**, *103*, 7441. (i) Nakao, Y. *J. Colloid Interface Sci.* **1995**, *171*, 386.

(12) (a) Liz-Marzán, L. M.; Giersig, M.; Mulvaney, P. *Chem. Commun.* **1996**, 731. (b) Liz-Marzán, L. M.; Giersig, M.; Mulvaney, P. *Langmuir* **1996**, *12*, 4329. (c) Kobayashi, Y.; Correa-Duarte, M. A.; Liz-Marzán, L. M. *Langmuir* **2001**, *17*, 6375.

(13) Kutsch, B.; Lyon, O.; Schmitt, M.; Mennig M.; Schmidt, H. *J. Non-Cryst. Solids* **1997**, *217*, 143.

(14) Bharathi S.; Lev, O. *Chem. Commun.* **1997**, 2303.

(15) Selvan, S. T.; Ono Y.; Nogami, M. *Mater. Lett.* **1998**, *37*, 156.

(16) Selvan, S. T.; Nogami, M.; Nakamura, A.; Hamanaka, Y. *J. Non-Cryst. Solids* **1999**, *255*, 254.

(17) (a) Duff, D. G.; Baiker, A.; Edwards, P. P. *Chem. Commun.* **1993**, 96. (b) Sarathy, K. V.; Raina, G.; Yadav, R. T.; Kulkarni, G. U.; Rao, C. N. R. *J. Phys. Chem. B* 1997, *101*, 9876.

(18) Turkevich, J.; Garton, G.; Stevenson, P. C. *J. Colloid Sci., Suppl. 1* **1954**, 26.

(19) Mason, M. G. *Phys. Rev. B* **1983**, *27*, 748.

(20) Yazawa T.; Kadono, K.; Tanaka, H.; Sakaguchi, T.; Tsubota, S.; Kuraoka, K.; Miya, M. *J. Non-Cryst. Solids* **1994**, *170*, 105.

(21) Tanahashi, I.; Tohda, T. *J. Am. Ceram. Soc.* **1996**, *79*, 796.

(22) Tanahashi, I.; Manabe, Y.; Tohda, T.; Sasaki, S.; Nakamura, A. *J. Appl. Phys.* **1996**, *79*, 1244.

(23) Bloemer, M. J.; Haus, J. W.; Ashley, P. R. *J. Opt. Soc. Am. B* **1990**, *7*, 790.

(24) Uchida, K.; Kaneko, K.; Omi, S.; Hata, C.; Tanji, H.; Asahara, Y.; Ikushima, A. J.; Tokizaki, T.; Nakamura, A. *J. Opt. Soc. Am. B* **1994**, *11*, 1236.

(25) Hache, F.; Ricard, D.; Flytzanis, C.; Kreibig, U. *Appl. Phys. A* **1988**, *47*, 347.

(26) Matsuoka, J.; Mizutani, R.; Kaneko, S.; Nasu, H.; Kamiya, K.; Kadano, K.; Sakaguchi, T.; Miya, M. *J. Ceram. Soc. Jpn.* **1993**, *101*, 53.